

# An electrically pumped germanium laser

Rodolfo E. Camacho-Aguilera,<sup>1</sup> Yan Cai,<sup>1</sup> Neil Patel,<sup>1</sup> Jonathan T. Bessette,<sup>1</sup>  
Marco Romagnoli,<sup>1,2</sup> Lionel C. Kimerling,<sup>1</sup> and Jurgen Michel<sup>1,\*</sup>

<sup>1</sup>Massachusetts Institute of Technology, 77 Massachusetts Ave., Cambridge, MA 02139, USA

<sup>2</sup>PhotonIC Corporation, 5800 Uplander Way, Los Angeles, CA 90230, USA

\*[jmichel@mit.edu](mailto:jmichel@mit.edu)

**Abstract:** Electrically pumped lasing from Germanium-on-Silicon pnn heterojunction diode structures is demonstrated. Room temperature multimode laser with 1mW output power is measured. Phosphorous doping in Germanium at a concentration over  $4 \times 10^{19} \text{cm}^{-3}$  is achieved. A Germanium gain spectrum of nearly 200nm is observed.

© 2012 Optical Society of America

**OCIS codes:** (140.2020) Diode lasers; (140.3380) Laser materials; (140.5960) Semiconductor lasers; (160.3130) Integrated optics materials.

---

## References and links

1. D. J. Lockwood and L. Pavesi, *Silicon Photonics* (Springer-Verlag, 2004).
2. M. E. Groenert, C. W. Leitz, A. J. Pitera, V. Yang, H. Lee, R. Ram, and E. A. Fitzgerald, "Monolithic integration of room-temperature cw GaAs/AlGaAs lasers on Si substrates via relaxed graded GeSi buffer layers," *J. Appl. Phys.* **93**(1), 362–367 (2003).
3. H. Park, A. Fang, S. Kodama, and J. Bowers, "Hybrid silicon evanescent laser fabricated with a silicon waveguide and III-V offset quantum wells," *Opt. Express* **13**(23), 9460–9464 (2005).
4. J. Liu, X. Sun, D. Pan, X. Wang, L. C. Kimerling, T. L. Koch, and J. Michel, "Tensile-strained, n-type Ge as a gain medium for monolithic laser integration on Si," *Opt. Express* **15**(18), 11272–11277 (2007).
5. J. Liu, X. Sun, Y. Bai, K. E. Lee, E. A. Fitzgerald, L. C. Kimerling, and J. Michel, "Efficient above-band-gap light emission in germanium," *Chin. Opt. Lett.* **7**(4), 271–273 (2009).
6. J. Liu, X. Sun, R. Camacho-Aguilera, L. C. Kimerling, and J. Michel, "Ge-on-Si laser operating at room temperature," *Opt. Lett.* **35**(5), 679–681 (2010).
7. G. Shambat, S.-L. Cheng, J. Lu, Y. Nishi, and J. Vuckovic, "Direct band Ge photoluminescence near 1.6  $\mu\text{m}$  coupled to Ge-on-Si microdisk resonators," *Appl. Phys. Lett.* **97**(24), 241102 (2010).
8. S.-L. Cheng, J. Lu, G. Shambat, H.-Y. Yu, K. Saraswat, J. Vuckovic, and Y. Nishi, "Room temperature 1.6  $\mu\text{m}$  electroluminescence from Ge light emitting diode on Si substrate," *Opt. Express* **17**(12), 10019–10024 (2009).
9. M. O. E. Kasper, T. Aguirov, J. Werner, M. Kittler, J. Schulze, "Room temperature direct band gap emission from Ge p-i-n heterojunction photodiodes," in *Proceedings of Group IV Photonics 2010* (2010).
10. X. Sun, J. Liu, L. C. Kimerling, and J. Michel, "Room-temperature direct bandgap electroluminescence from Ge-on-Si light-emitting diodes," *Opt. Lett.* **34**(8), 1198–1200 (2009).
11. J. Liu, X. Sun, L. C. Kimerling, and J. Michel, "Direct-gap optical gain of Ge on Si at room temperature," *Opt. Lett.* **34**(11), 1738–1740 (2009).
12. R. E. Camacho-Aguilera, Y. Cai, J. T. Bessette, D. Kita, L. C. Kimerling, and J. Michel, "High active carrier concentration in n-type, thin film Ge using delta-doping," submitted for publication (2012).
13. G. Scappucci, G. Capellini, W. M. Klesse, and M. Y. Simmons, "Phosphorus atomic layer doping of germanium by the stacking of multiple  $\delta$  layers," *Nanotechnology* **22**(37), 375203 (2011).
14. R. E. Camacho-Aguilera, Y. Cai, J. T. Bessette, L. C. Kimerling, and J. Michel, "Electroluminescence of highly doped Ge pnn diodes for Si integrated lasers," *Proc. 8th IEEE Intern. Conf. GFP, Vol. 190*, 10.1109/GROUP1.104.2011.6053759 (2011).
15. S. Xiaochen, L. Jifeng, L. C. Kimerling, and J. Michel, "Toward a Germanium Laser for integrated silicon photonics," *IEEE J. Sel. Top. Quantum Electron.* **16**(1), 124–131 (2010).

---

## 1. Introduction

It has been long acknowledged that a monolithically integrated laser for silicon (Si) based photonic circuits would be an enabling technology that could accelerate the implementation of silicon photonics significantly [1]. Early attempts to integrate III-V semiconductor lasers on a silicon platform had only limited success [2, 3]. More recently, germanium (Ge) has been suggested as a gain medium for lasing on Si [4]. Using a combination of tensile strain and n-type doping, efficient direct bandgap emission of Ge can be achieved [5]. Optically pumped

lasing in Ge was demonstrated using a Ge waveguide with polished facets [6]. Furthermore, attempts in electrically injection have demonstrated pin and pnn Ge diodes emitting between 1590 and 1700nm [7–10]. Here we present an electrically pumped pnn Ge diode laser that can be monolithically integrated into a CMOS process. These first laser devices produce more than 1 mW of output power and exhibit a Ge gain spectrum of over 200nm.

## 2. Experiments and results

Initial estimates of gain in n-type Ge based on experimental results showed that an n-type doping level of  $1 \times 10^{19} \text{cm}^{-3}$  would yield a gain of about  $50 \text{cm}^{-1}$  [11]. Such a gain can lead to lasing when pumped optically because optical losses are mainly limited to facet losses and free carrier losses in Ge. For electrical pumping, additional losses due to the electrical contacts, free carrier losses in doped poly Si and losses due to the interaction with the contact metal, have to be overcome. Modeling of mode propagation in Ge waveguides with electrical contacts shows that these additional losses are  $>100 \text{cm}^{-1}$ . To overcome by these losses, the Ge gain must be increased by increasing the n-type doping to a level of  $3\text{-}5 \times 10^{19} \text{cm}^{-3}$  [2]. Recently, we achieved n-type doping levels of  $> 4 \times 10^{19} \text{cm}^{-3}$  by using a delta-doping technique during epitaxial growth of Ge [12]. By correlation of photoluminescence (PL) intensity, n-type doping level, and measured material gain, we have determined that an n-type doping level of  $4 \times 10^{19} \text{cm}^{-3}$  corresponds to a material gain of  $>400 \text{cm}^{-1}$ , enough to overcome the losses in an electrically pumped laser device.

Ge waveguides of  $1 \mu\text{m}$  width were fabricated by selective growth of n-type Ge-on-Si in silicon oxide trenches using Ultra-High Vacuum Chemical Vapor Deposition (UHV-CVD) [3]. A delta-doped Ge layer was grown on top of the n-type Ge to serve as a phosphorous diffusion source [12, 13]. The delta-doping technique inserts monolayers of P in the Ge film at low temperatures by alternating the phosphine and germane gas flow in the CVD reactor. After thermal annealing to drive the phosphorous into the n-type Ge layer, the delta-doped Ge layer was removed during planarization using chemical mechanical polishing (CMP), to reach a uniform doping concentration in the gain medium. The remaining thickness of the Ge waveguide after CMP varied between 100 and 300nm depending on wafer and location on the wafer. Due to severe dishing of the waveguides after CMP the supported optical modes in the waveguides could not be determined exactly. Up to six cavity modes can be supported in the largest waveguides. An 180nm thick amorphous-Si film was then deposited via a Plasma-Enhanced CVD process and subsequently phosphorus-implanted to a doping level of  $10^{20} \text{cm}^{-3}$ . After a dopant activation anneal at  $750^\circ\text{C}$ , a metal stack, consisting of Ti and Al was deposited for top and bottom contacts. The oxide trench provides excellent current confinement. In order to assure even carrier injection into the n-type Ge, the top contact metal was deposited on top of the waveguide. After dicing, the waveguides were cleaved to expose the Ge waveguide facets. A thin oxide layer was deposited on the facets to protect against contamination and catastrophic optical mirror damage which was observed in devices that did not have oxide protection.

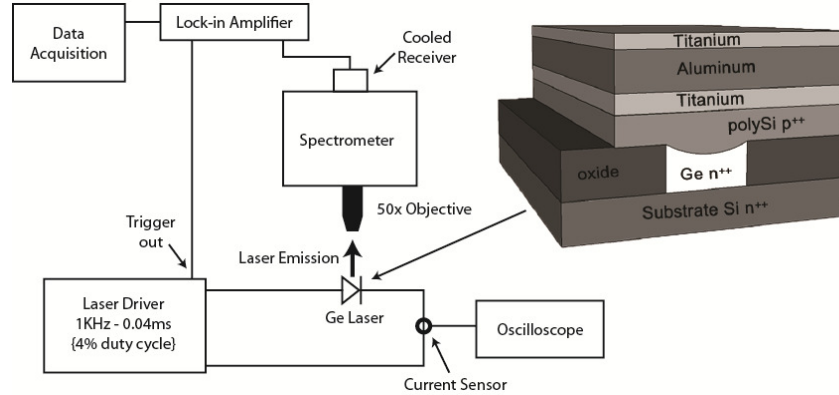


Fig. 1. Schematic of the measurement set-up.

The waveguide emission was measured using a Horiba Micro PL system equipped with a cooled InGaAs detector with lock-in detection. The emission power measurement was calibrated using light from a commercial 1550nm laser that was coupled into a single mode optical fiber with the fiber end at the sample location. In the calibration we verified that the detection was linear with input power. The electrical pumping was supplied by a pulse generator with current pulse widths in the range of 20  $\mu$ s to 100 ms. The duty cycle was varied between 2 and 50%, typically 4% to reduce electrical current heating effects. The laser was contacted with metal probes and the current was measured using an inductive sensor placed directly in the biasing circuit. The experimental set-up is shown in Fig. 1.

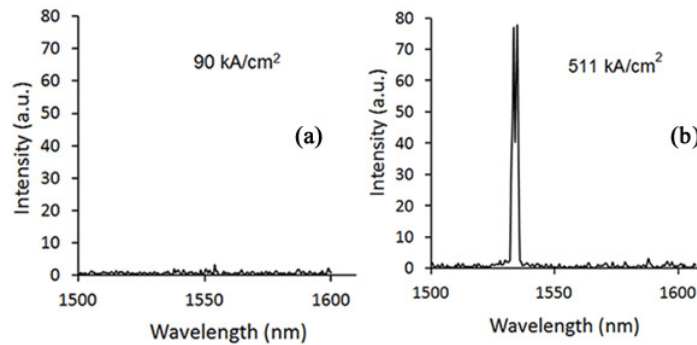


Fig. 2. Ge laser emission spectrum before (a) and after (b) threshold. The cavity length of the waveguide is 333 $\mu$ m and the waveguide height about 100nm. Current injection employed pulse widths of 50 $\mu$ s at 800Hz and 15°C. The detector spectral resolution was 1.2nm.

Figure 2 shows the spectrum of an electrically pumped Ge laser below and above threshold. The broad, direct band gap related electroluminescence spectrum, observed for highly  $-$ doped n-type Ge LEDs, has been reported earlier [14]. The spectra in Fig. 2 employed short integration times to assure wide spectrum analyses. Measurement time for these large laser devices is ultimately limited by metal contact breakdown due to the high current flow. Figure 2(a) shows no spectral features above the noise floor. When the injection current density is increased above threshold, sharp laser lines appear, as shown in Fig. 2(b). The observed linewidth of the individual lines is below 1.2nm, the spectral resolution of the measurement set-up. All measurements were performed with the samples mounted on a thermo-electric cooler at 15°C. Local device temperatures, however, are likely higher due to the high current injection but could not be reliably determined.

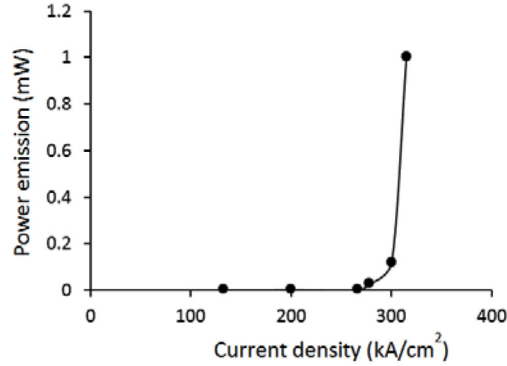


Fig. 3. L-I curve for a 270 $\mu$ m long waveguide device. 40 $\mu$ s electrical pulses were used at 1000Hz. Measurement temperature was 15°C.

Figure 3 shows the L-I spectrum for a typical electrically pumped Ge waveguide laser. The lasing threshold at about 280kA/cm<sup>2</sup> is clearly visible. This measurement was taken with the set-up in Fig. 1 using a wide instrumental spectral resolution of 10nm, at a wavelength of 1650nm, monitoring a single laser line. The number of datapoints is limited by metal contact breakdown at high current level. The optical emission power of about 1 mW corresponds to Fig. 3. Occasionally we observed up to 7 mW. The spectrum in Fig. 2 shows two lines. The estimate of the cavity free spectral range is 1nm, and the line spacing in Fig. 2, 3nm, is a possible multiple of the FSR.

These lasers show a dependence of emission wavelength on threshold current density that is consistent with the expected modal loss variation and that confirms the theoretical conclusions that the gain spectrum of Ge for the given doping level and strain reaches over more than 100nm spectral width [15]. For high doping levels of  $4 \times 10^{19} \text{cm}^{-3}$ , and tensile strain of  $\sim 0.2\%$ , we observed lasing in the range from 1520nm to 1700nm. Figure 4 shows selected laser lines between 1576nm and 1656nm for different Fabry-Perot cavities of the same gain material.

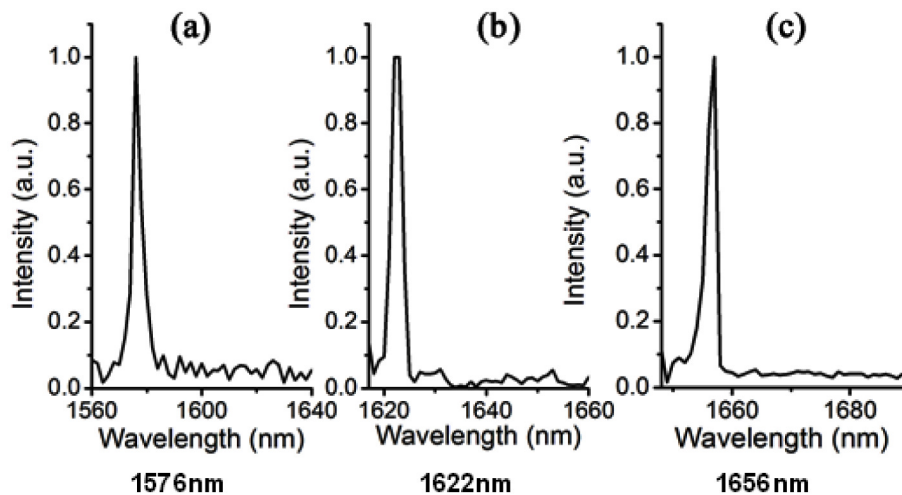


Fig. 4. Spectra of Ge lasers with different Ge waveguide heights. The measured laser line wavelengths are (a) 1576nm, (b) 1622nm, and (c) 1656nm.

The CMP-induced variation in cavity height provides self-consistent evidence of the wide gain spectrum and the gain clamping condition by lasing. Under lasing action optical gain (and population inversion) is clamped at exactly the value of the resonant cavity losses. In our

devices, the Ge waveguide height is directly related to the modal loss. Since Ge has the highest refractive index in our device structure, thinner Ge layers expel more of the resonant mode into the highly-doped poly-Si cladding and into the lossy metal contacts. The wavelength corresponding to the Ge gain peak (the threshold injection level) and the cavity loss is the expected emission wavelength of the device. As the modal confinement decreases with decreasing Ge layer thickness, modal loss and correspondingly threshold current increases and the emission wavelength blue shifts. In Fig. 5, we show spectral threshold conditions for two different modal cavity losses using a parabolic band model as described in [8].

A Ge waveguide of 300nm thickness has a modal loss of about  $90 \text{ cm}^{-1}$  due to losses in the doped poly Si and the metal electrode (solid line). A Ge waveguide of 100nm thickness, however, has a modal loss of about  $1000 \text{ cm}^{-1}$  due to the closer proximity of the mode to the electrode (dashed line). To overcome the high losses of the thin Ge waveguide, a relatively high carrier injection level is needed. Lasing is therefore expected at around 1520nm, close to what we find in Fig. 2. For lower loss waveguides we expect lasing to occur at longer wavelengths as shown in Fig. 4.

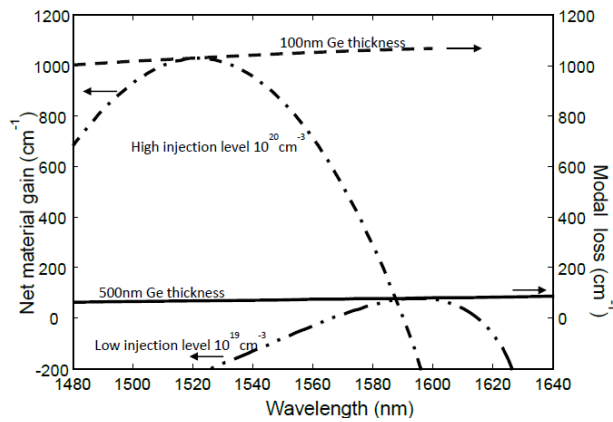


Fig. 5. Simulation of gain clamping condition for two different Ge waveguide thicknesses (100nm: solid line; 300nm: dashed line). The axes plot the corresponding modal loss and gain spectrum for the two different injection levels that are needed to overcome the respective modal losses and to achieve lasing.

### 3. Conclusions

We have observed lasing from electrically pumped n-type Ge Fabry-Perot cavities. The threshold current densities decrease with increased modal confinement. The emission linewidth is less than the 1.2nm resolution of our measurement. Laser emission wavelengths were observed between 1520nm and 1700nm with a variation consistent with the gain clamping condition for each device. Measured output powers greater than 1 mW at room temperature were measured. Improvements in the Ge growth, electrical contacts, and in modal loss reduction will decrease the lasing threshold to values comparable with Fabry-Perot diode lasers. The high power and observed gain spectrum of nearly 200nm indicate that the Ge laser could be used for WDM applications. Since the laser can be monolithically integrated into any CMOS process flow, novel device applications and systems can be developed.

### Acknowledgments

This work was supported by the Fully Laser Integrated Photonics (FLIP) program under APIC Corporation, supervised by Dr. Raj Dutt, and sponsored by the Naval Air Warfare Center - Aircraft Division (NAWC-AD) under OTA N00421-03-9-002. R.E.C.-A. was supported by a NSF Graduate Research Fellowship award number 1122374.